Numerical Structural Analysis of a Sailing Yacht Mast

Gabriel Alejandro Herrat Vieira
gabriel.herrat@tecnico.ulisboa.pt

Instituto Superior Técnico, Lisboa, Portugal

May 2022

Abstract

Due to the complexity of the mast and its structural system, it must be designed with attention to guarantee structural integrity and high performance. To fulfil those criteria, this study is based on research that makes use of the Sub modelling Technique in the Finite Element Method, analysing the behaviour of a sailing yacht mast made of carbon fibre and the structural elements that support it, along with a local strength approach, examining a specific region of the mast. From the technical point of view and as a result of the applied parametric study, it was concluded that the usage of thinner layers of stacked carbon fibre plies for the ply drop-off of the reinforcement patch can be beneficial for the stress distribution in the mast-forestay region. As a fundamental part of this project, the theoretical and engineering aid provided by the yacht spars company Rondal was vital. The structural analysis employed in this thesis promotes a detailed analysis that can be applied in several critical regions of the mast, allowing to create a mesh refinement in the region of interest to analyse local strength. Furthermore, this method enables simulating different design solutions for different structural components for optimisation. The methodology applied can be considered of great interest for the design process of the mast design industry.
Keywords: Mast, Submodeling, FEM, Rigging, Structural Analysis

1 Introduction

The objective of the dissertation is to create a structural analysis of a sailing yacht mast through the application of the Finite Element Method (FEM) and, more precisely, the implementation of the sub modelling technique available in the commercial software Abaqus.

A sailing yacht mast and the structure that support it are constantly subjected to a complex load throughout their entire operational life, either by the aerodynamic loads generated by the wind while sailing, by the inertial loads or by the load present on the rigging system.

In this thesis, the sub modelling technique is explored firstly in the preliminary study cases to get a profound understanding of the subject and applied afterwards on a mast with a 57 m in performing a global strength analysis and a local analysis on a critical region.

Applying numerical simulations in the design process becomes extremely important when an optimised structural solution is targeted. This has been proved in researches where FEM has been implemented for different purposes.

However, the most common implementation is beam elements with equivalent stiffness to assess the global strength and verify the compliance with classification society requirements.

This dissertation aims to establish a productive methodology for accurate global and local model analyses. More precisely, a global model of a sailing yacht mast and respective rigs, and submodels in the forestay lug perform a parametric study in the reinforcement design.

This type of approach allows creating a rational way to apply a mesh refinement in the region of interest locally. Throughout this research, it is presents a theoretical background of mast structures and submodelling techniques, followed by study cases related to sub modelling and, finally, the structural analysis of a 57 m sailing yacht mast with the respective results and conclusions.

2 Background

2.1 Sails and Rig System Interaction

When a sailing yacht is considered, it involves a complex system due to aerodynamic and hydrodynamic forces that constitute the equilibrium state and generate the propulsion of these vessels in different sailing conditions. The sails can create enough lift to overcome the drag of the hull. Nevertheless, the same force generated by the sails has a lateral component (perpendicular to the sails) that must be compensated by the righting moment of the hull, developed by the hull and keel's weight, principally. This lateral force equilibrium also can reduce the sway motion of the yacht. Figures 1 and 2 represent a graphical simplification the elementary forces present in the hull and

sails that generate propulsion in a sailing boat, with its components.

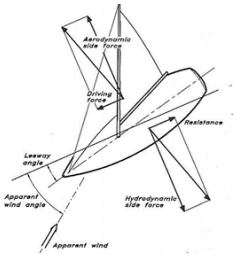

Figure 1: Elementary forces on a sailing yacht (upwind). [8]

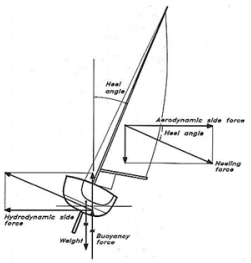

Figure 2: Transverse equilibrium of forces. [8]

The rig system can be described as a structure composed of beams and cables that support the loads generated by the sails. As the principal vertical structural component, the mast is subjected to axial, longitudinal and transverse loads; therefore, it is balanced and supported by the shrouds and stays. In simultaneous, the spreaders can reduce the unsupported length of the mast and increase its transverse stability. In addition, there are the fore and back stays (or runners) counteract the bending effect of spreaders and longitudinal deflection of the mast.

When it comes to strength stability, it has been observed that the buckling phenomenon mainly governs the limit states of rigging systems due to its slenderness. Despite that, ultimate strength, yielding and fatigue (e.g., in welded or bonded zones, turnbuckles, toggles, terminals and others) may also be considered.

In terms of mechanical properties requirements, the mast must be able to support the compression induced by stays and shrouds as a consequence of rig tunning as well as the aerodynamic loads.

2.1.1 Keel Stepped Mast and Deck Stepped Mast

The mast can be either stepped on the deck or stepped on the keel, and both of these alternatives can have their attributes and drawbacks. In the case of the keel stepped mast, it is a better solution in terms of structural integrity since the hull structure supports the mast. As a drawback, in this type of mast stepping, there is the space below the deck occupied by the mast, and if the deck opening is not well sealed, water can leak inside the hull.

In reference [8], it is stated that by letting the mast go through the deck and be stepped on the keel, the required moment of inertia can be reduced by 35%, which is beneficial for weight saving.

Regarding deck-stepped masts, these are generally positioned on metal support to ensure suitable mast attachment. From the perspective of sail trim, deck-stepped masts tend to be more flexible and easier to bend, meaning that the mast is better to optimise performance in diverse wind and sea conditions. These technical adjustments are essential in a racing context where small details can make the difference.

In the case of the study developed for this dissertation, a keel-stepped mast is analysed.

2.1.2 Mast Pretension

Apart from the tension generated by sails, the application of pretension on a sailing yacht rig system has great relevance when it comes to structural stability, safety and performance. By increasing the stiffness of the rig system when applying tension, the structure is more prevented from large displacements, keeping the structure stable and significantly improving the sail's aerodynamic performance.

Despite that, it is pretty complex to understand each rig system and how it should be tunned since each yacht is unique, principally for larger yachts. An iterative process often executes this based on practical knowledge and Finite Element Simulations to find the correct tension that should be applied in each rig and mast jack displacement.

2.1.3 Shrouds and Stays

As supportive structural elements, shrouds and stays allow a distribution of the stress on the mast, making the rig system stiffer and well supported. On the other hand, they will enable the application of the desired tension on the mast to achieve the desired mast curvature for performance and safety reasons. The main principle of the pretension is that only when the structure is entirely subjected to load, the leeward shrouds should just begin to slacken. In effect, in [2], it is provided, as a standard for rig scantlings, that the mast pretension must be performed to avoid slack in the leeward cap shrouds with an appropriate safety factor to avoid slack when sailing at angles equal to or lower than the Safety Working Angle, which is generally 30°.

It is noteworthy that stays and shrouds are explicitly designed to support tension loads. Thus the materials used may have adequate properties.

2.2 Spreaders

The spreaders have the critical role of reducing the unsupported length of the mast and increasing its transverse stability along with the shrouds. They are also helpful in obtaining a longitudinal pre-bend of the mast, with the contribution by the aft swept spreaders.

These structural elements are mainly loaded by compression created by the shrouds and are generally fitted in the mast allowing the rotation around the y axis, as shown in figure 3, to avoid having a bending moment acting on them. In contrast, the rotation

around the z-axis is blocked to prevent the mast from changing its curvature longitudinally.

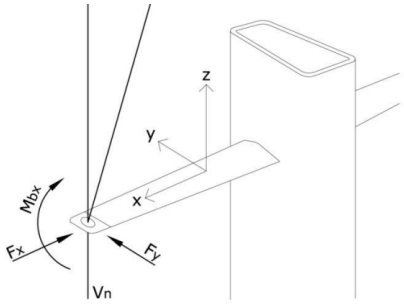

Figure 3: Shrouds and spreader connection with force and moment vector diagram. [10]

2.3 State of the Art

Due to the complexity and peculiarity of the subject, a significant share of masts and rigging systems design has been substantially based on empiric design criteria. Indeed, as mentioned in [11], significant uncertainties still affect the design loads applied and most of them are empirical. Only high-level competitions such as the America's Cup and unique projects for large yachts can afford the time and cost involved in these researches.

Implementing of numerical simulations for rigging systems in diverse contexts has become more frequent and convenient. Moreover, it has become a requirement in [2].

In literature [11], a study case is presented focused on the structural design of mast and rigging of sailing yachts from a practical point of view, stating how the equilibrium of yachts is traditionally analysed in a quasi-static state, considering that the aerodynamic forces equilibrate the vessel's righting moment. Moreover, it was underlined in [12] that despite the evolution of the aerodynamic and hydrodynamic fields thanks to prestigious investigations developed for international competitions, some problems remain with a question mark, such as the behaviour of rigging under wind gusts, the dynamic loading on the mast due to inertial loads caused by rough sea state and the pretension loads induced by the rig tunning.

In addition, in [5] can be found information regarding rig tunning procedures. It reviewed the application of pretension on a sailing yacht rig system, presenting a numerical validation while comparing with experimental results of the dock tunning of a 67 m mast.

Furthermore, in [6], the measurements taken from force transducers were investigated to compare with the results of a FEM analysis. The load cases considered in the computations were the dock pretension applied on the rig and sailing upwind with a 30^{o} heel angle.

In [3], a more profound evaluation of a mast deformation was elaborated, presenting a dynamic buckling analysis that was carried out for the bottom panel of a large sailing yacht. According to [4], the reigning limit state, global buckling can be simulated using the Euler eigenmode method on FEA with models composed of one-dimensional elements. The beforementioned type of analysis can be sufficient for normal scantling assessment procedures. Still, it might not be the case for performance analysis, which requires the structure's dynamic behaviour.

Moreover, in the approach [11], several methods and considerations for the different procedures applicable to the mast and rigging design are pointed out.

2.4 Approach to Structural Analysis

One possible way that engineers use to treat the analysis of complex structural components is by using coupled element approaches, however, to achieve this, it is important to be able to couple the element types that conform to the governing equations of the problem. In the literature [13], three different methods are provided to couple different types of elements (beam-solid, beam-shell and shell-solid) with the mathematical development that can be implemented in Abaqus as a command. Moreover, in [9] it is referred that for a global model made of shell elements, solid elements can replace the shells in the area of interest and be coupled to the surrounding shell elements either by applying the Mindlin-Reissner kinematic assumption or using a similar formulation like the one presented in [9] that allows considering the stretching of the shell thickness. An illustrative example of coupling for local mesh refinement can be seen in figure 4 a).

Although the coupling method can be effective, the complexity of the element combination in the same model appears since there are mathematical difficulties in the connections between the different elements due to the incompatibility in terms of degrees of freedom and the appearance of artificial stresses at intersected boundaries.

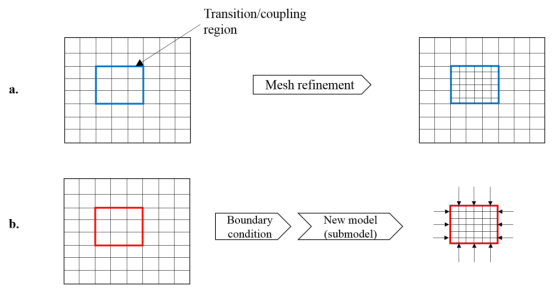

Figure 4: Two different methods to merge scales in FEA. [9]

The necessity of having accurate analysis to assist the design process with a more practical methodology encouraged us to consider the sub modelling technique

in Finite Element Analysis in this project. It can be employed various challenging tasks such as stress concentration, 3D crack propagation, contact analysis, fatigue analysis and others. It consists in using the solution of a coarse mesh model (global model) to provide boundary conditions for local and more refined analysis in a second model (submodel), as illustrated in figure 4 b).

The concept of sub modelling is sustained by St.Venant's principle that states "The difference between the effects of two different but statically equivalent loads become very small at sufficiently large distances from the load". This implies that applying a coarse mesh in a global model can provide results for a very refined local model as long as the boundary conditions are transferred sufficiently far away from the region of interest to ensure that these are not affected by the coarse mesh model inaccuracy in that region.

As referred to in [14], sub modelling can bring benefits in terms of computational time but must be applied correctly not to attract other sources of error. This study aims to define the effect that the submodel boundary location has on the convergence of the submodel solution.

In [1] it is presented a proposal for exploiting the potentiality of the sub modelling technique, applied to the simulation of wear by using different sub modelling techniques, varying in the quantity that was transferred (nodal forces, displacements and a combination of both). In the field of ship structures, the sub modelling method was applied effectively to the analysis of a large ship structure [7]. Additionally, in [15], a hybrid data + model-based sub-modelling (HDMS) method is prposed, which uses a sensor measurement on the preselected boundaries of a region of interest in a structure to drive the submodel by applying a force-based sub modelling procedure.

As for the different techniques implemented in sub modelling, the following are the most dominant and present in commercial software:

- **Displacement-based sub modelling** – consists in extracting the displacements from the solution of the global model, interpolating them and apply on the local model.
- **Stress-based sub modelling** - is also known as surface-based sub modelling. This technique interpolates the global stress field onto the submodel integration points on the driven element-based surface facets.

3 Sub Modelling Study Cases

A few different study cases were developed in this project to assess the effectiveness of sub-modelling to obtain accurate responses for the structural analysis. These study cases represent structural components in different circumstances of loading aiming to simulate simplified scenarios that are predictable in terms of their structural response.

The flat plates analysed had the dimensions and material properties shown in the tables below:

Length	1	[m]
Width	0.4	[m]
Thickness	0.05	[m]

Table 1: Plate dimensions.

E	70×10^9	[Pa]
ν	0.35	-

Table 2: Material Properties.

The first study case consisted in applying a compressive load on a flat plate to assess the effect of global model mesh refinement and submodel allocation in this method. In conclusion, it can be remarked from this study case that using the displacement-based sub-modelling technique, it must be taken into consideration the allocation of the submodel boundary since it can affect the accuracy of the results, as well as the global model mesh refinement. While displacement results easily match accurate results, the stress response can be conditioned by those two factors, principally near the boundaries of the submodel.

The second study case consisted of analysing a plate with a hole being compressed. The hole situated in the centre of the plate was created with a radius of 0.02 m. Once again, the stress and displacement results presented in this study case verified the advantage of using sub-modelling to assess the response of a certain region of interest to achieve an accurate and refined response.

Having the last study case present for comparison, the third study case was developed to assess the effectiveness of applying sub-modelling to a structural component that has suffered a geometry change from the global model to the submodel. This concept is sustained by using of a simplified global model solved with a coarse mesh to obtain a global response. Afterwards, that global response is used to apply in the region of interest with a more detailed 3D modelling to optimise the structure or elaborate a local analysis.

To elaborate on this study case, it was considered the same plate geometry, material properties, boundary conditions and element size for the global model and submodel as in the former case, with the exception that the global response was obtained from a plate without a hole and only afterwards, in the submodel, the hole was added. In the result analysis, stress and displacement results were presented, and

the calculation of the relative deviation with respect to study case 2.

In conclusion, although very close, the results are slightly underestimated when this technique is employed. However, this underestimation is not worrying when the change in geometry is considerably small as the one implemented and proved by the relative deviation calculations.

4 Mast Structural Analysis

The structural analysis of a sailing yacht mast was elaborated using sub-modelling techniques in FEA software Abaqus. As a result of the work developed with Rondal, a global model (GM) of a mast was developed, including its standing rigs and spreaders according to the design and structural configuration conceived by the company. Moreover, submodels were designed with a parametric variation in the patch reinforcement to create a local and more detailed analysis of the forestay-mast connection. The load condition consists in applying pretension on the mast and the maximum allowable backstay load since it generates the most critical load state in the region where submodelling was used. The objective of this analysis consisted in obtaining accurate analysis of the mast behaviour, followed by assessing the stress response generated by the different designs created for the ply drop-off in the reinforcement patch of the forestay lug and the usage of different element types.

4.1 Finite Element Models

It was developed a global model including a shell element mast tube that was assembled afterwards with the other structural components that connect to the mast and interact with it, that includes the longitudinal stays, vertical and diagonal shrouds and four spreaders on each side of the mast, all modelled with beam elements. The submodels were specially modelled with the reinforcement patches and simulated in both shell and solid elements, resulting in six submodels.

4.2 3D Models

Firstly a global model was created, including all the necessary components. Afterwards, the submodels were made based on the global model region selected for the local analysis. From technical drawings provided by Rondal, the mast was designed and three-dimensionally represented by its mid surface considering the tapering present near the top and the geometrical allocations of the relevant fittings such as the spreaders, longitudinal rigs, shrouds and deck level for its posterior assembly.

For the submodels, the geometry of the global model was fragmented relatively to the point of intersection between the forestay and the mast. Two horizontal planes at a distance of 1500 mm from the forestay-mast connection point define the longitudinal extremities of the submodels, while the other extremities are characterised by a plane offset from the back face of the mast at a distance of 250 mm. Additionally, the reinforcement patches were designed as rectangular surfaces of different sizes, representing stacked plies of carbon fibre (also called blocks) that are laid upon the inner surface of the mast.

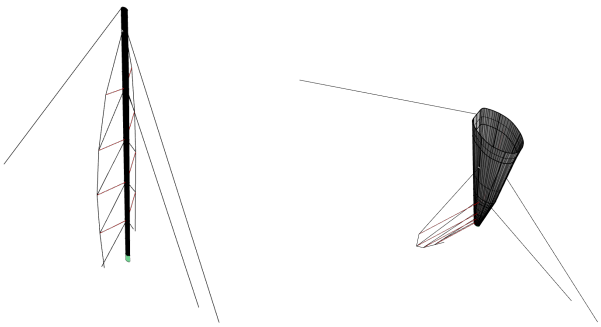

(a) GM modelled in Rhinoceros (b) Forestay-Mast connection

Figure 5: Global Model - Mast surface with rig system scheme.

Three different patch arrangements were considered:

- **Submodel 1 (SM1)** - Reinforcement patch with five blocks of 10 layers; ply drop-off spacing of 30 mm in the cross-sectional direction and 60 mm in the longitudinal direction.
- **Submodel 2 (SM2)** - Reinforcement patch with ten blocks of 5 layers; ply drop-off spacing of 30 mm in the cross-sectional direction and 60 mm in the longitudinal direction.
- **Submodel 3 (SM3)** - Reinforcement patch with ten blocks of 5 layers; ply drop-off spacing of 15 mm in the cross-sectional direction and 30 mm in the longitudinal direction.

It is worth mentioning that this was designed considering that each layer of carbon thickness is 0.3 mm.

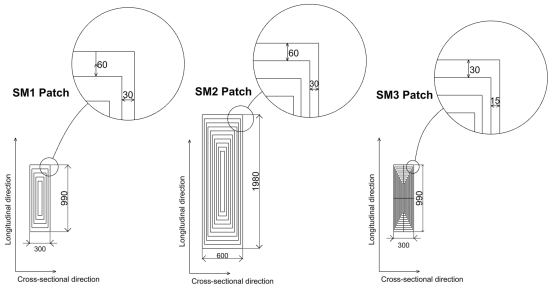

Figure 6: Submodels patch arrangement.

Henceforward the submodels will be referred to as their element type followed by the initials enumerated above, i.e., Shell SM1, Shell SM2 and Shell SM3, for the submodels to be analysed with shell elements and Solid SM1, Solid SM2 and Solid SM3 for the submodels to be analysed with solid elements.

4.3 Material Properties

The mast being analysed in this project was designed in carbon fibre. As a material for this type of structure, it brings numerous advantages in strength, performance and weight saving. The laminate lay-up required to build this type of structure is of high complexity and involves applying a significant number of carbon fibre plies as part of the production process.

The complexity of the composite lay-up led defining the mechanical properties as an anisotropic material, based on common values of carbon fibre reinforced plastic (CFRP) used in the industry with the characteristics shown in Table 3.

Table 3: Material Properties.

Property	Mast CFRP	Solid Carbon	Unit
E_{xx}	125×10^9	180×10^9	Pa
E_{yy}	25×10^9	10×10^9	Pa
E_{zz}	25×10^9	10×10^9	Pa
ν_{12}	0.3	0.3	-
ν_{13}	0.3	0.3	-
ν_{23}	0.04	0.04	-
G_{12}	6×10^9	6×10^9	Pa
G_{13}	6×10^9	6×10^9	Pa
G_{23}	5×10^9	5×10^9	Pa

The same material properties were defined for the mast components and spreaders (Mast CFRP in Table 3).In contrast, the material Solid Carbon was attributed to the rigs that constitute the rest of the structure.

4.4 Interactions and Boundary Conditions

To obtain an accurate behaviour of the models, interactions were introduced to connect the structural components that constitute them. Additionally, boundary conditions were presented so that it stimulates the attachment of the rigs and mast to the yacht's deck as well as the mast pretension and backstay load. In the case of the submodels, the respective boundary conditions were applied to transfer the loads obtained from the global model.

The boundary conditions applied to the structure simulate the attachment of the structure to the yacht's deck using pin constraint. The pretension of the mast was obtained through a simplification that consisted in creating a pin constraint in the cap shrouds and applying vertical displacement imposed on the mast-step with a magnitude of 200 mm, pushing the mast upwards as a way of simulating the hydraulic mast jack. Additionally, the backstay maximum allowable load (25 tons) was applied to the structure. An additional boundary condition imposed was the deck displacement constraint in the horizontal plane, representing the hole in the deck that constitutes a support point of the mast.

4.5 Finite Element Mesh

This modelling step had to be meticulously executed, creating the required conditions for the mesh to be made the most efficiently. That included the creation of partitions in the geometries, selecting the element size and seeding critical regions of the parts to ensure nodal allocations in desired places. Obtaining a suitable arrangement of the elements in the most uniform way with appropriate aspect ratios is crucial to achieving accurate results in FEA.

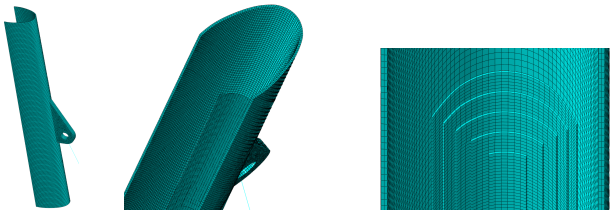

(a) (b) (c)

Figure 7: Solid SM1 Mesh.

The element type selected for the shell submodels was S4R (4 node shell element), while in the solid submodels, the hexahedral solid element was used (C3D8R: An 8-node linear brick, reduced integration).

4.6 Results

The post-processing consisted of the extraction of results to assess a variety of aspects such as the global model structural behaviour, the correlation between the global model and submodels, submodels stress distribution in the most critical regions to analyse the different stress components throughout the reinforcement patch and the evaluation of the parametric variation.

4.6.1 Global Model

The response results from of a complex interaction between all of its components. However, there is an expected behaviour based on practical knowledge and the arrangement of the rigs that support the mast.

Although in reality, the desirable deformation of the mast would be with a slight backward deformation, in this case, it wasn't entirely achieved due to the simplification created for the pretension process. Most certainly, the application of multiple pre-defined tensions on the upper diagonal and vertical shrouds si-

multaneously with the displacement of the mast step would lead to the desired response. Despite that, the global model exhibited an accurate behaviour of the structure.

Additionally, the load generated by the backstay, pushing the tip of the mast to the aft, clearly created a bending effect on the higher part of the mast, causing tension in the forward face of the mast and compression in the back face of the mast.

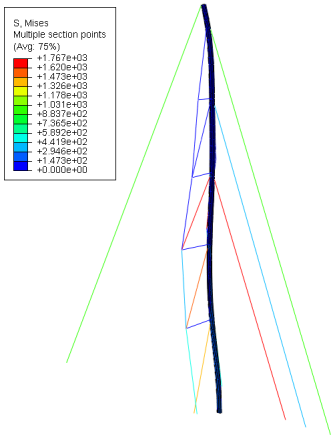

Figure 8: Von Mises Stress on Global Model

Nodal displacements were extracted at the same location in the global model and submodels to validate the displacement results. To do this, two cross-sections of reference were considered to extract the results in the different models. This led to conclude that the stiffness of the global model and submodel correlated.

From the displacement results, it was observed that the global model and submodel correspond to similar responses, having a maximum deviation of 0.8% and 0.7% for the two reference cross-sections selected.

4.6.2 Submodels

To make visible the most critical regions of the structure considering different stress components, it was important to observe the stress distribution along the submodel's length (longitudinal) and in the cross-sections that intersect with the patch in different regions.

Figure9 (b) shows an example of the cross-sections for a better understanding.

Submodel 1

From the response of the submodel, it was concluded that the main component in the resultant stress state comes from the normal stress generated by the backstay load. It is also visible that the reinforcements create a decrease in the stress as the ply drop

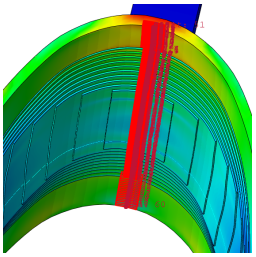

(a) Longitudinal path on Solid SM2.

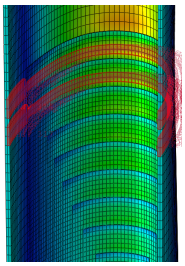

(b) Example of cross-section paths in Solid SM2.

Figure 9: Examples of paths created for submodels' result analysis.

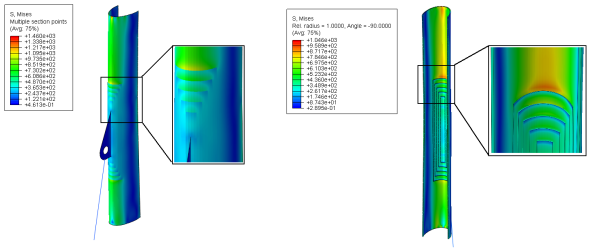

(a) Von Mises Stress in Shell SM1.

(b) Von Mises Stress in Solid SM1.

Figure 10: Von Mises Stress results in Submodel 1 (Shell and Solid elements).

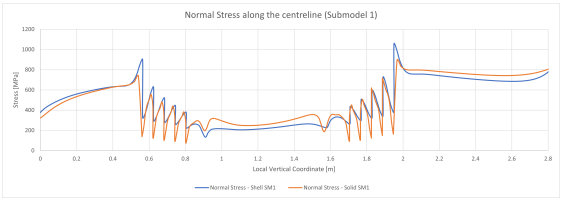

Figure 11: Normal Stress along longitudinal path of Submodel 1.

off thickness increases, as was expected, and a low stabilised stress value in the lug region. Comparing the results obtained from the shell element submodel and solid element submodel, it can be seen that, although the behaviour is very similar, the solid elements compute a drop in the stress value considerably higher than the shell submodel.

This submodel presented a maximum normal stress drop (variation) of approximately -563 MPa for the shell submodel and -661 MPa for the solid submodel at the local vertical coordinate of 1.95 m, the location of the highest extremity of the reinforcement patch.

Besides normal stress, in-plane shear stress and peel stress in the edges of the reinforcement blocks were analysed. In the case of the shear stress, cross-sectional results were extracted from the model to observe this stress distribution as shown in the following

graphs:

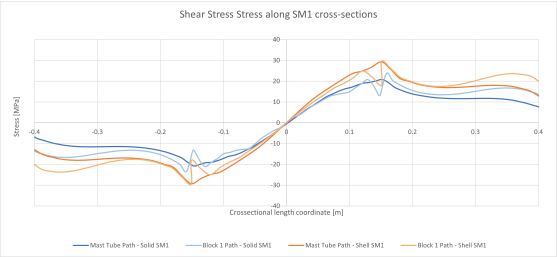

Figure 12: In-plane Shear Stress in selected cross-sections of Submodel 1.

Figure 12 represents shear stress in the most critical region of the reinforcement patch. It is visible that the presence of the reinforcement creates peaks in the shear stress distribution, and these sudden peaks are found principally in the locations where the thickness varies. Comparing the element types used, it is evident that the solid element submodel computes higher variations in the stress values when the thickness changes.

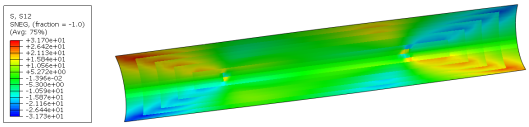

Figure 13: In-plane Shear Stress pattern in reinforcement patch (SM1).

In figure 13 it can be visualised with more detail the shear stress pattern in the reinforcement patch isolated.

In addition, a study of the peel stress (via the normal stress component in the perpendicular direction of the surface) was created. This is a frequent topic of study in composite components, principally in components built separately and bonded during the assembly process. Figure 14 shows the results obtained on the edges of the reinforcement patch plies:

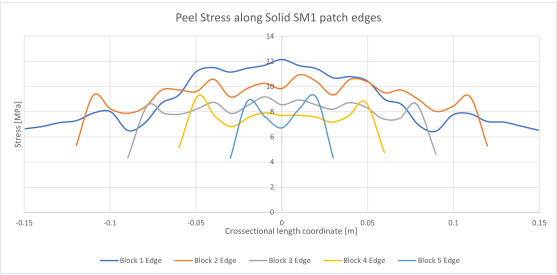

Figure 14: Peel Stress distribution in patch plies edges (SM1).

The edges of the reinforcement plies selected to represent the results belong to the uppermost extremity of the reinforcement patch (above the lug), more precisely, in the leading edges of the ply drop-off (15).

In the graph presented in figure 14, the peel stress results present positive values through all the lengths of the edges, meaning that the stress state creates an effect of 'pulling' the plies of carbon in the edges due to the load condition of the mast, reaching a maximum of approximately 12.2 MPa for the outermost carbon ply. It should be also noted that, besides the analysis of peel stresses the ply drop-off, it was noticed that in the area of the lug-reinforcement connection, peel stress results reach the highest values, achieving a maximum of 54.9 MPa in the upper extremity of the lug as shown in figure 16. This is naturally caused by the tension generated in the forestay as a consequence of the load applied in the backstay, pulling the lug downwards.

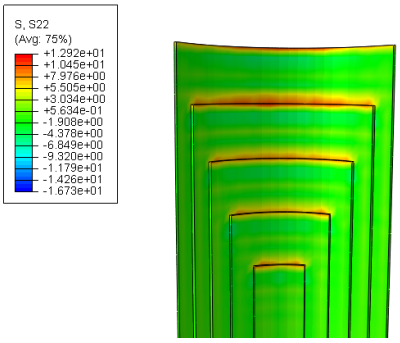

Figure 15: Peel stress in ply drop-off (SM1).

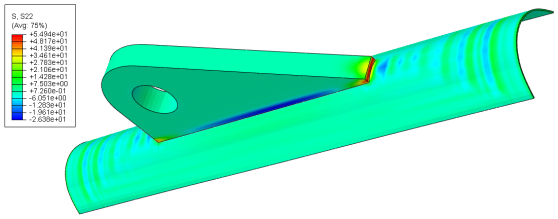

Figure 16: Peel Stress in lug-reinforcement connection (SM1).

Submodel 2

This submodel was designed to maintain the same spacing between the ply drop-off as in Submodel 1 but applying thinner blocks of stacked carbon layers. In this case, the reinforcement is composed of 10 blocks of 5 layers each, having a drop-off thickness of 1.5 mm at each block.

As expected, the present submodel behaves similarly to as the latter submodel analysed but with more reinforcement blocks.

The results obtained for the longitudinal distribution of Normal Stress show the stress peaks generated

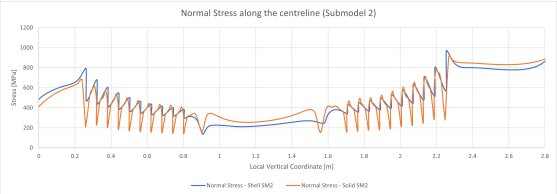

Figure 17: Normal Stress along longitudinal path of Submodel 2.

by the reinforcement change in thickness(figure 17), just as in the former submodel.

Once again, it was verified that the shell element submodel computed slightly higher stress values than the solid element submodel. Moreover, the solid element submodel encountered a higher amplitude of stress drops due to the reinforcement drop-offs. The maximum amplitude observed for the normal stress drop was located in the patch reinforcement's uppermost extremity with a magnitude of -368 MPa and -598 MPa in the shell and solid submodels, respectively.

Regarding the shear stress, it was selected the cross-sections in the upper extremity of the reinforcement patch for its analysis.

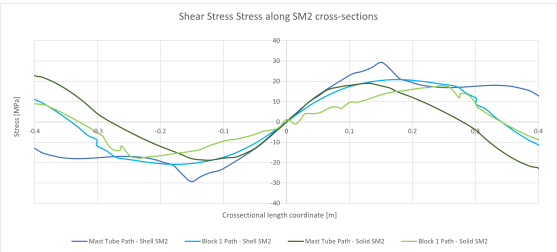

Figure 18: In-plane Shear Stress in selected cross-sections of Submodel 2.

From the results obtained from the In-plane Shear Stress it can be observed once again the influence of reinforcement patch has on this stress component. In figure 18, it can be observed that the usage of thinner carbon blocks decreases the variation of shear stress. Furthermore, the cross-sectional coordinate (horizontal axis on the graph) where the maximum shear stress magnitude is achieved resembles those observed in Submodel 1. It was also noticed that the shear stress pattern in the reinforcement was similar to the one obtained in the previous submodel, despite the changes in geometry.

Once again, peel stress was assessed in the leading edges of the ply drop-off, a region of interest for this stress component.

In the graph present in figure 19, the peel stress results present positive values through the length of the edges that were selected as verified in the previous submodel and reaching a maximum of 7 MPa in the

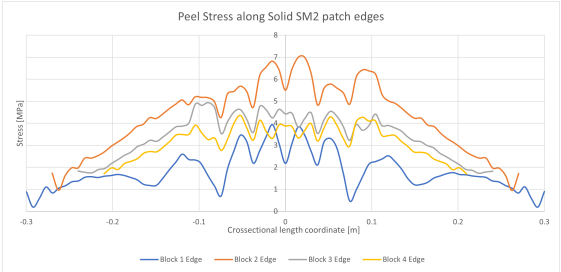

Figure 19: Peel Stress distribution in patch plies edges (SM2).

edge of Block 2 (blocks are enumerated from the outside to the inside of the reinforcement). In contrast with submodel 1, this submodel presented a considerably lower level of peel stress. It's relevant to mention that the graph shown above only represented four of the studied edges since these gave the most relevant results and allowed us to visualise the response better.

Just as observed in the former submodel, in the region of the lug-reinforcement connection, the peel stress results reach the highest values, achieving a maximum of 82.2 MPa in the upper extremity of the lug as shown in figure 20.

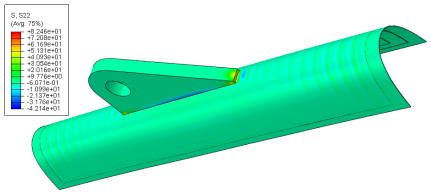

Figure 20: Peel Stress in lug-reinforcement connection (SM2).

Submodel 3

As the final submodel, it was opted to create an arrangement of the patch reinforcement with a smaller spacing in the blocks of the ply drop-off while maintaining the drop-off thickness used in Submodel 2.

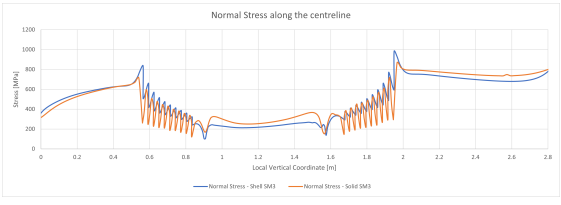

Figure 21: Normal Stress along longitudinal path of Submodel 3.

The Normal Stress in the graph in figure 21 has a similar distribution along the longitudinal path of the submodel. The successive stress variations visible on

the locations of the ply drop-off are stress changes due to the thickness variation that, on one hand, are distributed through a smaller distance when compared to Submodel 2. On the other hand, the observed gaps are smaller in amplitude, achieving a maximum value of -363 MPa and -523 MPa of stress drop. This is a smaller variation than the one noticed in the submodels previously presented.

Moreover, the results were plotted using the cross-section paths to analyse the shear stress in the cross-sections.

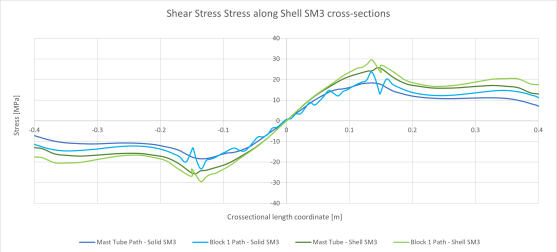

Figure 22: In-plane Shear Stress in selected cross-sections of Submodel 3.

In the shear stress graphs shown in figure 22 the variation in shear stress is notable due to the reinforcement patch that varies in thickness. The behaviour of the in-plane shear stress is similar to the other submodels and the stress pattern. However, it can be observed that the variation of stress through the drop-off happens more suddenly due to the smaller spacing between each block.

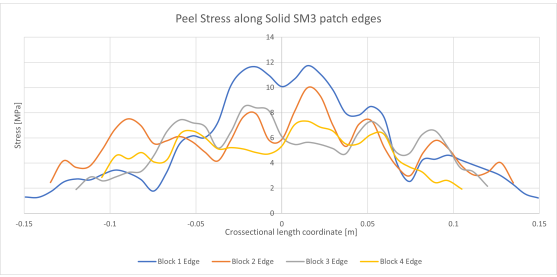

Figure 23: Peel Stress distribution in patch plies edges (SM3).

As a final analysis, the peel stress results are compared with the other two submodels.

In the graph in figure 23, the peel stress results present positive values through all the lengths of the edges as verified in the previous submodels and reach a maximum of 11.4 MPa for the outermost ply, i.e., the block that's is directly bonded to the mast tube. On the other plies, a decrease in the values of peel stress was observed.

Just as in submodel 2, the results presented in figure 23 belong to the four more relevant edges. Moreover, in the area of the lug-reinforcement connection, it was verified, once again, the highest results for this stress component, achieving a maximum of 72.2 MPa in the upper extremity of the lug.

From the three peel stress analysis performed, considerable differences in the results for the three submodels were observed. Submodel 1 and submodel 3 presented similitude in the patch reinforcement area, behaving similarly in the maximum peel stress values obtained at the edge of contact between block one and the mast tube. On the other hand, submodel 2 obtained lower values of peel stress in ply drop-off edges.

To finalise the mast analysis, a few conclusions should be taken. Firstly, a significant difference in normal stress distributions was noticed in the different designs produced for the reinforcement patches.

On the other hand, the in-plane shear stress had similar behaviour in the three submodels. Although a change in the stress peaks was noticed due to the ply drop-off, the global behaviour for shear stress resembled in the three submodels. Finally, the magnitudes of the results obtained for the normal stress in the submodels were considered moderately high. They can be allocated above the admissible limit considering the values that are acceptable (up to 800 MPa) by the composite manufacturer of the mast being studied. However, the results are still in the correct order of magnitude and allowed us to understand of the structural analysis and the implications of the parametric variation.

5 Conclusions

The present study allowed to create an approach for a structural analysis of a sailing yacht mast and its rigs, based on the fundamentals used to design this type of structure and implementing the FEA sub modelling technique to assess the structure locally. This way of modelling creates a rational method to analyse different design solutions and is very engineering-oriented, creating opportunity to study more complex topics such as crack propagation, contact wear and many others.

From the literature found related to this type of structure, it was concluded that each scientific research presents its challenges due to the singularity of each mast design and loading conditions. In addition, in the industry and from existing scientific research, the benefits of Finite Element Analysis have been verified to design spars and rigging systems to improve components in terms of strength and performance.

This research was elaborated in partnership with the composite and spars design company Rondal and allowed to achieve the goals set throughout its elaboration and fulfil the expectations created for the results.

In this project, three design solutions were presented in the submodels, using shell and solid elements to analyse the stress distribution and the re-

inforcement patch. Having that as the main focus of analysis, the third solution (Submodel 3) turned out as the one that presented the most reliable option and presented a smoother stress transition, showing stress peaks with less amplitude. It was also verified that using thinner layers of carbon in the reinforcement to define the ply drop-off is beneficial in decreasing the high stress gradients.

As additional recommendations, there are a few subjects of interest for future research, such as modifying the shape of the reinforcement using curved edges to improve the shear stress concentration and introducing more detail in the pretension process. Furthermore, alternative solutions to this detailed structural analysis could be made, such as the applying of shell-to-solid coupling, using mixed-dimensional elements in the same model, or implementing adaptive mesh refinement tools.

Acknowledgements

I want to express my gratitude to my professors for the transmitted knowledge, especially to Professor Yordan Garbatov and Engineer Marco Nawijn for providing this opportunity.

As a fellow from the scholarship funded by the family Soares dos Santos, I want to transmit my profound gratitude for the unconditional support and the opportunities created for me during this academic journey.

References

[1] C. Curreli, F. D. Puccio, and L. Mattei. Application of the finite element submodeling technique in a single point contact and wear problem. *International Journal for Numerical Methods in Engineering*, 2018. doi:10.1002/nme.5940.

[2] DNVGL. *Design and Construction of Large Modern Yacht Rigs I*, 2016. Part4, Ch.2, Sec. 1.

[3] M. Gaiotti and C. M. Rizzo. Dynamic buckling of masts of large sail ships. *Ships and Offshore Structures*, 10(3):290–301, 2015. doi: 10.1080/17445302.2014.887175.

[4] Germanischer Lloyd, Hamburg (Germany). *Rules & guidelines I ship technology – part 4, rigging technology*, 2009.

[5] S. Ghelardi, A. Garavaglia, C. M. Rizzo, and M. Paci. On the rig dock tuning of large sailing yachts. *Ocean Engineering*, pages 384–397, 2019.

[6] G. Grabe. The rig of the research sailing yacht "dyna" measurements of forces and fea. 1^{st} *High Performance Yacht Design Conference*, December 2002.

[7] M. Kitamura, H. Ohtsubo, A. Akiyama, and K. Bandoh. Submodeling analysis of ship structure with superconvergent patch recovery. *International Journal of Offshore and Polar Engineering*, 2003.

[8] L. Larsson, R. Eliasson, and M. Orych. *Principles of Yacht Design*. Bloomsbury Publishing, 2000.

[9] C. Möller and O. Sundlo. Method for merging scales in finite element analysis. Master's thesis, Chalmers University of Technology, Gothenburg, Sweden, 2017.

[10] P. Ploé. Scantling of sailing yacht mast and sail deformation simulation using finite elements. Master's thesis, University of Liege and Ecole Centrale de Nantes, February 2012.

[11] C. Rizzo and D. Boote. Scantling of mast and rigging of sail boats: a few hints from a test case to develop improved design procedures. 11^{th} *International Symposium on Practical Design of Ships and Other Floating Structures*, 2010.

[12] A. Shenoi, R. Beck, D. Boote, P. Davies, A. Hage, D. Hudson, K. Kageyama, J. Keuning, P. Miller, and L. Sutherland. Report of committee v.8, sailing yacht design. In 17^{th} *International Ship and Offshore Structures Congress*, volume 2, pages 456–470, 2009.

[13] K. W. Shim, D. J. Monaghan, and C. G. Armstrong. Mixed dimensional coupling in finite element stress analysis. *Engineering with Computers*, pages 241–252, 2002. doi:10.1007/s003660200021.

[14] M. W. Sracic and W. J. Elke. Effect of boundary conditions on finite element submodeling. In *Nonlinear Dynamics*, volume 1, pages 163–170. Conference Proceedings of the Society for Experimental Mechanics Series, 2019.

[15] B. Valeti and S. N. Pakzad. Hybrid data + model-based submodeling method for a refined response estimation at critical locations. *Structural Control and Health Monitoring*, 2020. doi:10.1002/stc.2646.